Modelling and Optimization of the NO Formation in an Industrial Glass Furnace

M. G. Carvalho
Associate Professor

V. S. Semião
Research Assistant.

P. J. Coelho
Assistant Professor.

Mechanical Engineering Department,
Instituto Superior Técnico,
Av. Rovisco Pais,
1096 Lisboa Codex,
Portugal

The effects of combustion excess-air level, air preheating, and fuel composition on the nitric oxide emissions from an industrial glass furnace are studied through the use of a mathematical model. The mathematical model is based on the solution of the time-averaged form of the governing conservation equations for mass, momentum, energy, and chemical species. The k-ϵ turbulence model is employed for modelling the turbulence fluxes. The flame is modelled as a turbulent diffusion one and the chemical reactions associated with the heat release are assumed to be fast. The fluctuations of scalar properties are accounted for by use of a clipped-Gaussian probability density function. The thermal radiation, playing the dominant role in the heat-transfer process, is modelled using the discrete transfer method. Because of the high temperatures at which industrial glass furnaces operate a considerable amount of thermal NO is formed. The present work presents a model, based on a chemical kinetic approach, to predict the nitric oxide emissions from industrial glass furnaces. The Zeldovich mechanism, retaining the reverse reactions, is incorporated in the model in order to predict the instantaneous NO net formation rate from atmospheric nitrogen. The whole procedure is applied to a cross-fired regenerative furnace. A set of parametric studies is carried out, demonstrating the ability of the model to evaluate the influence of changes in operating conditions on the NO emissions.

1 Introduction

1.1 Preamble. Combustion and pollution have been somewhat synonymous topics since mankind's discovery of fire. As a result of concerted, worldwide concern over the past two decades, for what is being emitted to the environment via the smokestack and the tail pipe, great strides have been made toward burning fuels cleanly. The steadily increasing severity of emissions regulations has been leading to much research on the chemistry of pollutant formation mechanisms, namely on nitric oxide emissions. Present day concerns of NO control address issues of fuel nitrogen release, the nature of fuel nitrogen species, interactions of nitrogen-containing species in fuel-rich combustion, radical overshoots in flames, conversion of the NO to NO_2 in gas turbines and gas burners and the reduction of NO.

Increasing pressure has been placed on engineers to develop theoretical and experimental methods able to quantify and enhance the industrial furnaces performances. Particularly acute is the need to comply with more stringent ecological requirements, by lowering the noxious gas emission without sacrificing production. Prediction codes capable of computing the aerodynamics, mixing, combustion, and thermal radiation in gas fired combustors to a reasonable degree of accuracy exist. However, these predictive tools have been far from sufficiently employed as a means of permitting the knowledge of emissions reduction control to be directly applied in the quest for improved burner and combustor designs. The large amount of air preheat and consequent elevated flame temperature in many industrial furnaces yield high levels of thermal NO emissions which is a cause of mounting international concern. The Portuguese glass industry is a particularly important national energy consumer and the restraints of recent legislation on pollutant emissions have turned the attention of engineers towards the importance of improving the combustion equipment design. Reductions in NO emissions are achievable through combustion modifications and to some extent through optimization of operating conditions, but parametric trials on full scale equipment are very expensive and accurate measurements are difficult. The number, and so the cost, of trials required to be performed could be considerably reduced with the aid of a reliable mathematical model.

The present paper describes the application of a full three-dimensional mathematical model to a glass melting furnace of the Portuguese industry. The turbulence, combustion, and radiation physical models are those used previously by the authors in order to optimize the performance of an industrial glass furnace [1] and they were extensively validated for another glass furnace [2]. These works did not include any model for the prediction of NO formation. Recently, a model was developed in order to predict the formation of the thermal NO from atmospheric nitrogen. This model was described in [3]

Contributed by the Production Engineering Division for publication in the JOURNAL OF ENGINEERING FOR INDUSTRY. Manuscript received Oct. 1989. Associate Technical Editor: S. G. Kapoor.

where it was applied to the prediction of nitric oxide emissions from a cross-fired regenerative furnace at standard operating conditions. In the present work this model is used in order to demonstrate its ability to evaluate the influence of changes in operating conditions on the NO emissions.

1.2 The Kinetics of NO Formation. The major portion of NO_x in practical systems has been found to be NO [4]. Consequently, the greatest number of analytical and experimental studies have been focused on NO formation. Nitric oxide may be built up from different ways:

(*a*) NO formation from atmospheric nitrogen is meant to specify the NO formed in combustion systems in which the original fuel contains no nitrogen atoms chemically bound to other elements. As this NO forms only at high temperatures it is called the *THERMAL NO*.

(*b*) NO formation from fuel-bound nitrogen is meant to specify the NO formed from the fuel compounds that contain nitrogen atoms bound to other atoms (generally carbon and hydrogen atoms). The NO formed from fuel-nitrogen species is referred to as *CHEMICAL NO* or *FUEL-BOUND NO*.

The numerous pathways of both complex mechanisms of NO formation may be found in the work of Levy [5].

A third and controversial mechanism for NO formation is termed "*PROMPT*" *NO*. The work on this subject has shown that in the flame zone the atmospheric nitrogen forms small quantities of cianotic compounds which are subsequently oxidized to NO.

The kinetics of NO formation from atmospheric nitrogen has been extensively studied [6]. Early investigations by Zeldovich et al. [7] determined the mechanism of NO formation in combustion of fuel-oxygen-nitrogen mixtures. However, Fenimore [8] has reported that, in the vicinity of the combustion zone, NO formation rates exceed those predicted by the Zeldovich mechanism. Rapidly formed NO, termed "*PROMPT*" *NO*, was supposed to accumulate from reactions between nitrogen and CH radicals followed by oxidation. More recent studies on kinetics of NO formation in laboratory flames support the Zeldovich mechanism (see [9]–[11]) and justify the above referred excess of NO formation by the presence of radicals in levels above their equilibrium values. According to Peters et al. [12], prompt NO contributes between 10 to 30 ppm in hydrocarbon flames while thermal NO may contribute up to several hundred ppm. In lean and near-stoichiometric flames the larger NO formation rates are primarily the consequence of superequilibrium concentrations of O and OH [13]. In fuel-rich flames, superequilibrium O and OH concentrations may account for some increase in the NO formation rate, but there is increasing experimental evidence that reactions between hydrocarbon species and molecular nitrogen play a significant role in NO formation (see, e.g., [13], [14]). Miller et al. [6] illustrated the transition from the prompt NO mechanism to the thermal mechanism in premixed methane/air flames as conditions become leaner. They show that when the equivalence ratio decreases from 1.37 to 1.06, the NO formation mechanism decreases from completely hydrocarbon/nitrogen to predominantly thermal.

In order to clarify the relevance of the prompt NO, Hayhurst et al. [15] performed measurements in premixed laminar flames of $H_2/O_2/N_2$, with a very small amount of various hydrocarbons, and they derived a simple formula for predicting the quantity of prompt NO in flame gases (within limits of temperature and stoichiometry). Drake [16] performed similar experiments in hydrocarbon turbulent jet flames and he concluded that prompt NO is an important mechanism for NO formation, resulting in up to 70 percent of the NO formation. However, as pointed out by Turns et al. [17], these measurements are not definitive proof that prompt NO plays a dominant role in hydrocarbon jet flames, since the addition of even small amounts of CH_4, as in Drake's experiments, substantially alters the stoichiometric ratio of the fuel, and hence, the flame length. Turns et al. estimate that in Drake's experiments flame lengths increase by 17 percent and 30 percent, respectively, for 3 percent and 6 percent CH_4 addition to the $CO/H_2/N_2$ fuel.

It can be concluded that prompt NO contributes to NO formation in hydrocarbon flames. The contribution of prompt NO is more significant in fuel-rich flames and, therefore, it can be important in fuel-rich eddies of turbulent diffusion flames (see, e.g., [18]). However, the relative importance of prompt NO decreases with temperature increase (see, e.g., [6], [14]) and it seems justifiable to neglect its contribution in glass furnaces where very high temperatures are achieved.

1.3 The NO Modelling in Practical Systems. The modelling of NO formation in practical combustion chambers has been a matter of research for the past two decades. Katsuki et al. [19] developed a two-dimensional mechanistic model to study the NO formation rate and its dependence on temperature and species concentrations in a gas turbine combustor using the Zeldovich mechanism. The calculations of the combustion aerodynamics were based on the simplified hypothesis of boundary layer approximation in the main flow region, nonreversed flow outside the recirculation zone, a single step and equilibrated reaction of fuel oxidation, absence of radiative heat transfer effects, and turbulence modelled by an empirical correlation. Exploiting the fact that NO is formed in a narrow region around the maximum temperature in turbulent diffusion flames, Peters [20] determined the NO formation rate by an asymptotic expansion in terms of a small parameter δ, using the Zeldovich mechanism. A two-dimensional axisymmetrical model was used and the predictions agree favorably with experimental results of a hydrogen-air jet diffusion flame, in spite of the use of an empirical correlation for the turbulent viscosity calculations. Jones et al. [21] developed a three-dimensional model using the Favre-averaged forms of the governing conservation equations, with the two-equations k–ϵ model for turbulent transport, to predict a gas-turbine combustor. The combustion model was based on the fast kinetics approach and fluctuations in scalar properties were accounted for by use of a Beta probability density function. Radiative heat-transfer was not accounted for and the Zeldovich mechanism was employed. Comparisons with experimental values have surprisingly shown that the model overestimated the NO concentrations although the possibility of super-equilibrium of radicals was not allowed for. Drake et al. [22] used a similar approach but a new kinetic model was presented for the pro-

Nomenclature

k_i = forward constant rate of reaction i

k_{-i} = reverse constant rate of reaction i

m_{NO} = time-mean *NO* mass fraction

S_{NO} = time-mean source term of the *NO* mass fraction transport equation

u_i = time-mean velocity component on the x_i direction

$[X]$ = concentration of the chemical species X (mole/m^3)

Γ_{NO} = effective diffusion coefficient for the *NO* mass fraction

ρ = time-mean density of the mixture

duction of NH_2. Ahmad et al. [23] used a model similar to the previous ones but the soot spatial distribution was also calculated. The model was applied to the calculations of a turbulent-jet diffusion flame. The importance of simulating the influence of turbulence on the chemical kinetics was shown in their work.

In spite of the numerous works on NO modelling, their application has almost always been restricted to gas turbines combustors and diesel engines. Nevertheless, a model to predict the NO emissions from an industrial glass furnace together with the three-dimensional simulation of the furnace under real operating conditions was presented in [3]. Time-averaged forms of the governing conservation equations along with the k-ϵ turbulence model were used. The combustion model was based on the fast kinetics hypothesis and turbulent fluctuations of scalars were accounted for by use of a Gaussian probability density function. Radiative heat-transfer was modelled using the discrete transfer method. The time-averaged NO mass fraction was calculated by solving its conservation transport equation. The Zeldovich mechanism was employed in order to calculate the NO formation rate and, for the first time, the reverse reactions were retained.

The present study extends the work [3] to the prediction of the NO emissions from a Portuguese industrial glass furnace. The combustion excess-air level, the air-preheating, and the fuel composition were varied in the present work to study their effect on the NO production rate and NO emissions.

1.4 Description of the Furnace. Figure 1 shows a sketch of the furnace, which is of the cross-fired regenerative kind. This furnace is essentially a large insulated container in which the batch enters via the doghouse wall and the molten glass exits from the opposite end. The firing ports are located along the sides of the furnace. There are four ports on each side, each port containing two fuel jets. The furnace is fired alternately from either side to ensure as uniform a heat flux to the glass as possible and to permit the regeneration process. The combustion products pass through regenerators that are used to preheat the combustion air, before it enters the furnace, to produce higher temperatures and heat fluxes to the glass. The wall openings surrounding the burners serve alternately as air entry locations and waste gas exits, as the firing direction is altered. Methane fuel is burned with 10 percent of excess air for normal operating conditions. The crown of the furnace and the side walls are refractory lined.

2 The Physical Modeling

The mass, momentum, energy, and chemical species transport equations for a turbulent three-dimensional reacting flow were applied in their cartesian co-oordinate form.

The two-equation model (see [24]), in which equations for the kinetic energy of turbulence k and its dissipation rate ϵ are solved, appears to be satisfactory for the present kind of application (e.g., [25]).

The combustion model is based on the idea of a single step and fast reaction between the gaseous fuel and the oxidant, assumed to combine in stoichiometric proportion. It was also assumed that all species and heat diffuse at the same rate, and hence the instantaneous gas composition can be determined as a function of a conserved scalar variable (see [26]). Any conserved scalar may be chosen and here the mixture fraction f, defined as the mass fraction of fuel present, both burnt and unburnt, was used.

In a turbulent flow, the mixture fraction will fluctuate and knowledge of its mean value is insufficient to allow the determination of the mean values of such quantities as density and temperature because of the nonlinearity of the relationships. A statistical approach to describe the temporal nature of the mixture fraction fluctuations was adopted. The time-

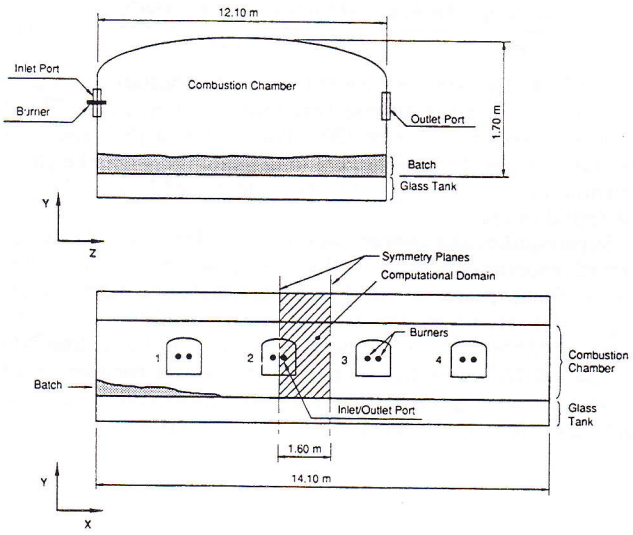

Fig. 1 A sketch of the furnace

averaged value of any property ϕ solely dependent on f can then be determined from the convolution of ϕ and the probability density function. The "clipped" normal probability density function for the mixture fraction, which is completely defined by its mean value, f, and variance, g, was employed (see [27]). The variables, f and g, also obey modelled transport equations.

The discrete transfer radiation prediction procedure [28] was utilized in this study. This procedure is numerically exact and applicable to arbitrary geometries. It is based on the solution of the fundamental radiative transfer equation within discretized solid angles. This last feature is of particular importance in the real world of geometrically intricate combustion chambers. The gas absorption coefficient was calculated from the "two grey plus a clear gas" fit of Truelove [29]. Water vapor and carbon dioxide are the prime contributors to the gaseous radiation.

As NO is present only in trace quantities, when compared to other species concentrations, and it has negligible influence on the heat releasing reactions and temperature, its calculations were performed independently of those for the combustion aerodynamics. At high temperatures, say in the range 1900–2500 K which is the case for glass melting furnaces, the thermal NO builds up by slow reactions when compared with the combustion ones and thus, the modelling of NO presumes a finite rate reaction. The usual assumption of chemical equilibrium made for the combustion model is not valid. The formation of NO is several orders of magnitude slower than the main heat release reactions and thus it is kinetically limited.

The time-mean NO mass fraction is calculated from the solution of the following transport equation:

$$\frac{\partial}{\partial x_i}\left(\rho \overline{u}_i \overline{m}_{NO}\right) = \frac{\partial}{\partial x_i}\left(\Gamma_{NO}\frac{\partial \overline{m}_{NO}}{\partial x_i}\right) + \overline{S}_{NO} \qquad (1)$$

The time-averaged source term $\overline{S}_{NO}$ is found by convoluting the instantaneous NO formation rate and the probability density function. The value of the instantaneous NO formation rate is obtained from the Zeldovich mechanism:

$$N_2 + O \rightleftarrows NO + N \qquad (R1)$$

$$O_2 + N \rightleftarrows NO + O \qquad (R2)$$

Furthermore, invoking the steady state assumption for the nitrogen atom concentration and assuming partial equilibrium for the formation reactions of the oxygen atoms-[0]- the instantaneous NO formation rate is given by (see, e.g., [9], [13], [18]):

$$\frac{d[NO]}{dt} = \frac{2[O]\,(k_1 k_2 [O_2][N_2] - k_{-1} k_{-2} [NO]^2)}{k_2[O_2] + k_{-1}[NO]} \qquad (2)$$

where k_1 and k_2 are the forward reactions constant rates and k_{-1} and k_{-2} are the reverse reactions constant rates. These constants were taken from [30]. The values of $[N_2]$ and $[O_2]$ are taken from the equilibrium values calculated by the combustion model. Details of the above described NO model can be found in [3].

Superequilibrium concentrations of radicals have been observed experimentally in well-stirred reactors, laminar premixed flames, laminar, and turbulent diffusion flames (see, e.g., [31]). However, the assumption of equilibrium for the O-atom concentration has been often used in modelling NO formation from practical combustion systems because of its simplicity (see, e.g., [12], [13], [21]). It is more realistic at high pressures, lean mixtures (see, e.g., [18], [21]) and high peak flame temperature (see, e.g., [6], [31]). According to [32], nonequilibrium effects may account for no more than a 25 percent increase in thermal NO_x, although there is no agreement about this figure [31]. Since there is an uncertainty in the rate constant for the Zeldovich reaction (R1) estimated to be ±35 percent ([33], [34]), and because in glass furnaces combustion takes place with excess air and the peak flame temperature is close to 2500 K, the assumption of equilibrium for the O-atom concentration was used in the present work.

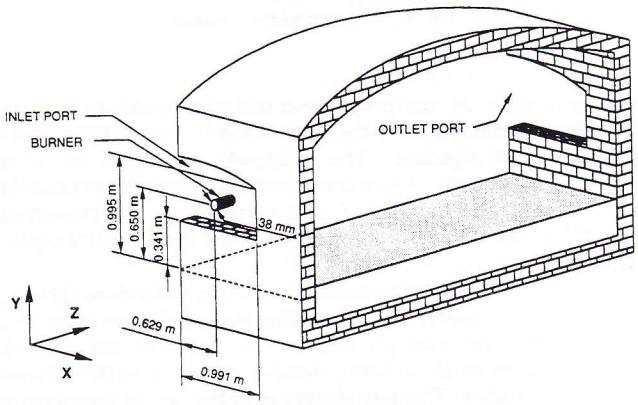

Fig. 2 The computational domain

3 The Numerical Solution Procedure

3.1 Some Computational Details. The present prediction procedure was applied for the solution of the process in a full scale industrial glass furnace under real operating conditions (see Fig. 1). The daily production of the glass is 10^5 Kg. The fuel is injected at 1400 K. For the standard case (10 percent of excess air) the total mass flow of fuel is 320 Kg/h. A prescribed glass temperature distribution was used.

Nearly all industrial furnaces are three-dimensional and exhibit the disparity of scales, in that most of the combustion takes place within a volume surrounding the burner which occupies only a small region of total furnace volume, but requires a disproportionately large portion of the total computational grid. Moreover, in the burners region the flame is generally almost insensitive to the details of the flow elsewhere in the furnace. These features suggest that the assumption of symmetry about cross-sectional planes, either bisecting the burner or the gap between them, as shown in Fig. 1, is reasonable [25]. This assumption which is probably not far from truth was used in the present work. If end effects were important or if the inlet conditions differed significantly from one port to another the calculations would have to be extended to the entire furnace. This could easily be accomplished by means of an iterative solution procedure as described and used in [1], but at the expense of a significant increase in CPU time. In the present case, the inlet conditions are identical for all

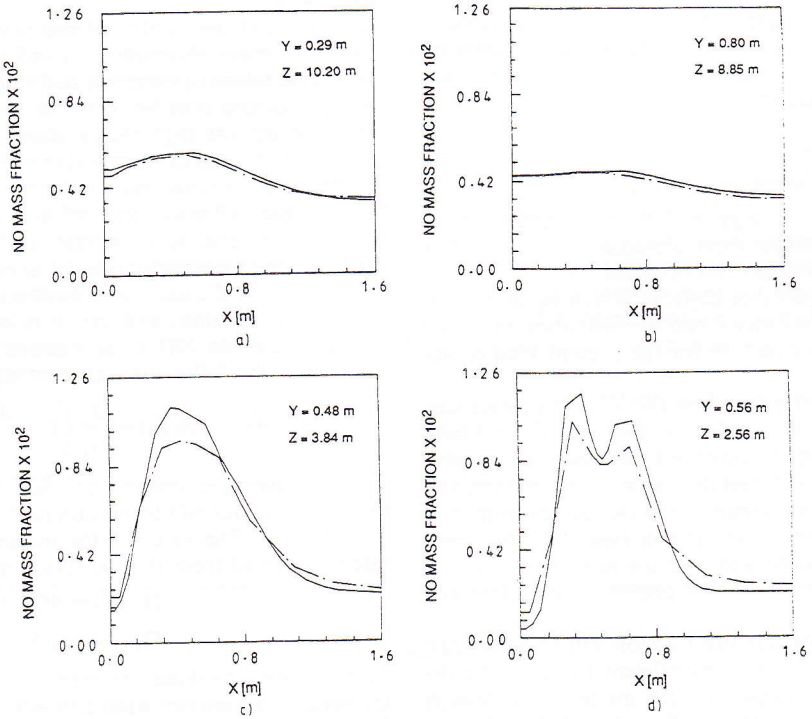

Fig. 3 NO mass fraction profiles [$Kg_{NO}Kg_{mix}^{-1}$] inside the furnace
— · — · — 11 × 14 × 14 grid nodes
——— 27 × 28 × 14 grid nodes

Table 1 The parameters under investigation

Run	Grid Nodes (x, y, z)	Excess Air (%)	Preheating (K)	Fuel Composition	Parameter under Investigation
1	11x14x14	10	1513	CH_4	
2	27x28x14	10	1513	CH_4	Grid Sensitivity
3	27x28x31	10	1513	CH_4	
4	27x28x31	5	1513	CH_4	Excess Air
5	27x28x31	0	1513	CH_4	
6	27x28x31	10	1413	CH_4	Air Preheating
7	27x28x31	10	1613	CH_4	
8	27x28x31	10	1513	86% CH_4 + 14% N_2	Fuel Composition

the ports and therefore the computational domain was restricted to the region limited by two symmetry planes and shown in Fig. 1. Therefore, the calculation domain, sketched in Fig. 2, is confined to a region limited by a pair of adjacent symmetry planes, the furnace walls, the glass surface, and the crown. A Cartesian grid was used with the curved surface of the crown replaced by a horizontal surface located at a level chosen in such a way that the volume remains the same.

Due to the long period of the alternating firing-direction cycle, the transient nature of the firing process was neglected.

Three different grids with $11\times14\times14$, $27\times28\times14$, and $27\times28\times31$ grid nodes (Runs 1, 2, and 3, respectively) were used in order to evaluate the sensitivity of the results to the grid refinement. The present study was aimed at the improvement of the actual operating conditions of the furnace, as far as the pollutant emissions are concerned. The effect of the combustion excess-air was analyzed by reducing its value from 10 percent to 5 percent and 0 percent (Run 3, 4, and 5, respectively). The influence of the air preheating was evaluated in Runs 6 and 7 in which the inlet air temperature was decreased to 1413 K (Run 6) or increased to 1613 K (Run 7). Finally, the influence of the fuel composition was studied in Run 8. The parameters investigated in this work are summarized in Table 1.

3.2 Method of Solution. The finite volume/finite difference method used to solve the equations entails subdividing the calculation domain into a number of finite volumes or "cells." The convection terms are discretized by the hybrid central differences/upwind method. The velocities and pressures are calculated by a variant of the SIMPLE algorithm. The solution of the individual equations sets is obtained by a form of Gauss-Seidel line-by-line iteration.

4 Results and Discussion

Validation of numerical predictions by means of comparison with experimental data acquired in a full-scale industrial glass furnace is a very important task. However, measurements are very difficult to obtain due to the severe conditions of high temperature and corrosion levels inside the furnaces and there is no data available for the glass furnace studied here. In spite of the lack of good quantitative validation evidence, the trends in the results show that the performance of this furnace is well-characterized by the mathematical model. In the numerical treatment of this furnace, some sources of inaccuracy may be present. The interaction between two neighboring flames is neglected. The application of the hybrid central differences/upwind scheme may lead to numerical diffusion. However, the numerical errors and the shortcomings of the turbulence and combustion models have proved to be of minor importance in previous applications. Indeed, the models used herein are the same used in a previous study [2], where extensive validation of the predictions against experimental data acquired in a real furnace was made. The results have shown good agreement between both. This is a consequence of the importance of the radiation in the large industrial furnaces.

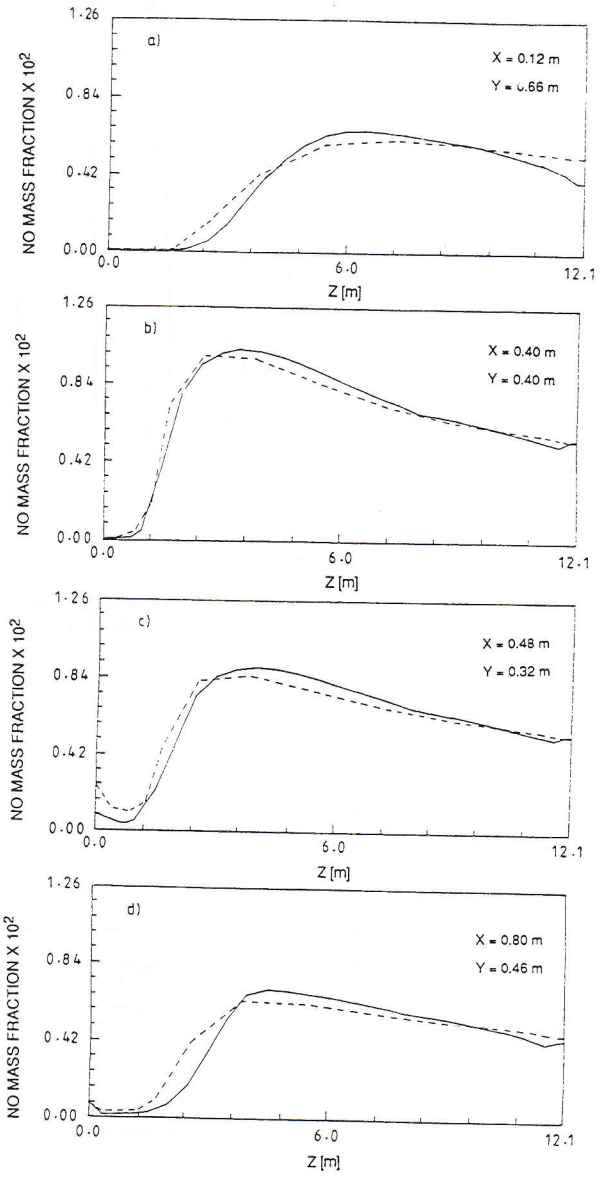

Fig. 4 NO mass fraction profiles [$Kg_{NO}Kg_{mix}^{-1}$] inside the furnace
----- 27 x 28 x 14 grid nodes
— 27 x 28 x 31 grid nodes

4.1 The Grid Dependence Tests. The first attempt to study the dependence of the results with the grid was directed to its refinement along the x and y directions (see Fig. 1). Selected results of this study are depicted in Fig. 3. This figure shows NO mass fraction profiles along the x direction (length of the furnace) for two different grids: $11\times14\times14$ nodes (Run 1) and $27\times28\times14$ nodes (Run 2). While panels (a) and (b) show the dependence of the results with the grid refinement in a region downstream the flame front, panels (c) and (d) show the same dependence in the flame front region. These results show that the NO mass fraction profiles exhibit negligible differences between the grids in regions downstream the flame front. Conversely, the profiles appear rather sensitive to the grid in the near flame-front zone due to the appearance in the calculations of details of the flow not previously detected.

Secondly, the dependence of the results with the grid refinement along z direction (see Fig. 1) was searched for and the results are displayed in Fig. 4. This figures contains NO

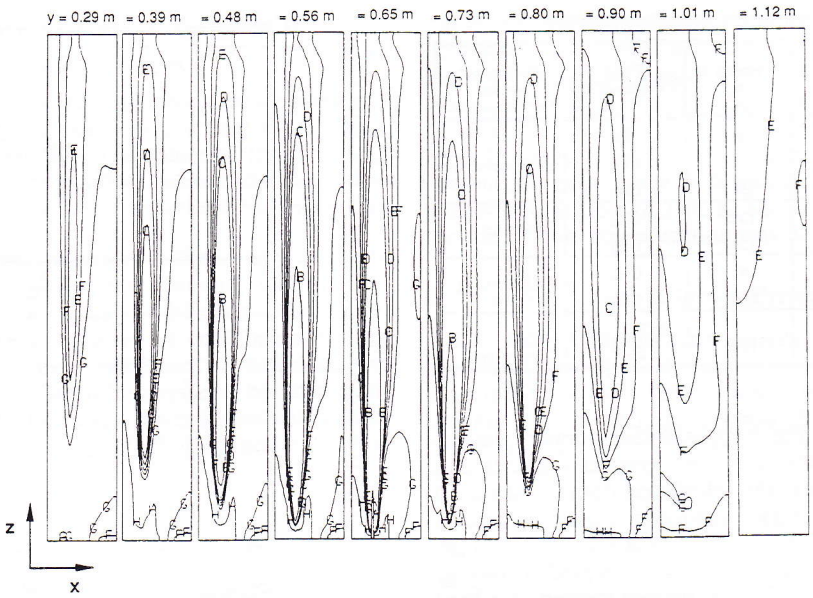

Fig. 5 Mixture fraction contours at several horizontal planes (A-0.50, B-0.10, C-0.07, D-0.063, E-0.057, F-0.05, G-0.04, H-0.02)

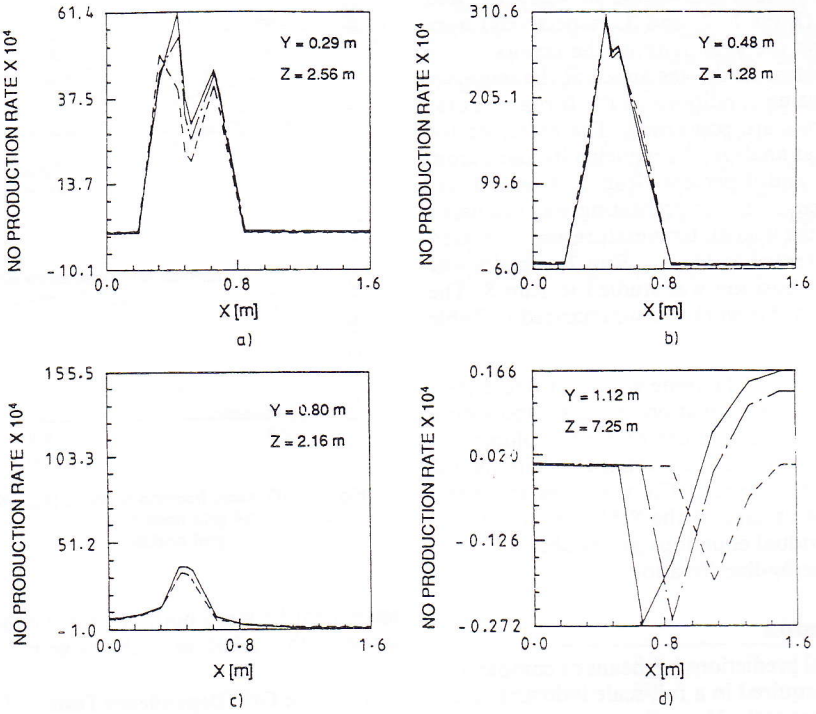

Fig. 6 NO production rate profiles [$Kg_{NO}m^{-3}s^{-1}$] inside the furnace
—— 10 percent of excess air
—·—·— 5 percent of excess air
····· 0 percent of excess air

mass fraction profiles along this direction (width of furnace) for two different grids with $27 \times 28 \times 14$ nodes (Run 2) and $27 \times 28 \times 31$ nodes (Run 3). These results show that the average NO mass fraction profiles do not display significant differences for both grids employed.

From the selected profiles shown in Figs. 3 and 4 it can be concluded that there is only a small degree of dependence of the predicted results on the grid refinement. The NO mass concentration at the outlet section does not change significantly for the grids used, and this is the important parameter, as far as pollutant NO emissions are concerned. In fact, the predicted average outlet NO concentrations for Runs 1, 2, and 3 are 3499, 3432, and 3346 kg/m^3, respectively, corresponding to a change of less than 5 percent between the maximum and minimum values. Therefore, as far as the objectives of the present paper are concerned, the grid used in Run 3 may be considered fine enough and was used in the parametric study that follows.

4.2 Standard Operating Conditions. Contours of the predicted mixture fraction at standard operating conditions are displayed in Fig. 5 for several horizontal planes. The region shown in these plots corresponds to the computational domain

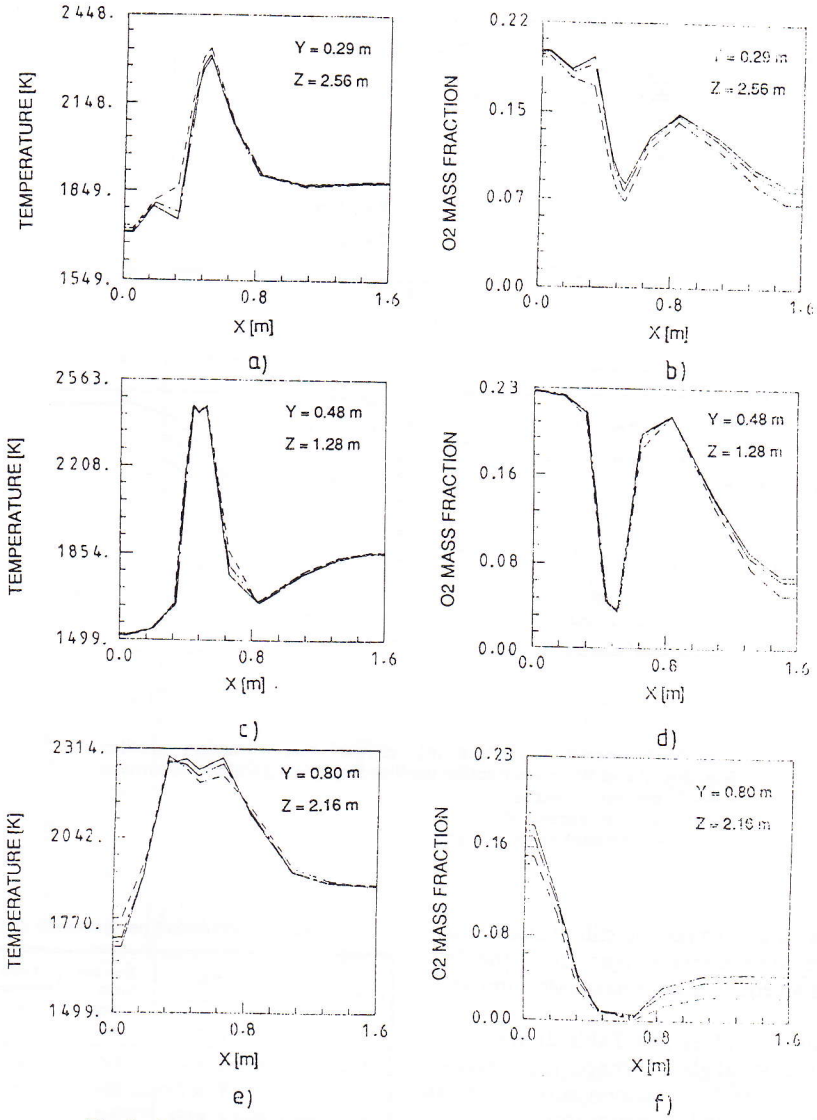

Fig. 7 Temperature profiles [K] and oxygen mass fraction profiles [Kg_{O2} Kg_{mix}^{-1}] inside the furnace
—— 10 percent of excess air
—·—·— 5 percent of excess air
····· 0 percent of excess air

sketched in Fig. 2. The stoichiometric mixture fraction is 0.055 for pure methane fuel. High values of mixture fraction are present near the burner as shown in the plane passing through its axis (y = 0.65 m). The mixture fraction decreases progressively as combustion takes place towards the outlet port, the glass surface and the crown of the furnace.

Figures 6 and 8 show some predictions for different levels of excess-air (see Table 1). Standard operating conditions correspond to 10 percent excess-air (Run 3).

In the horizontal plane y = 0.29 m, close to the glass surface, the maximum NO production rate occurs for the profile z = 2.56 m displayed in Fig. 6(a), that is in the fuel-lean edge of the flame front (see Fig. 5). This maximum corresponds to a region where high temperatures occur and significant oxygen mass fraction is present [see Figs. 7(a) and 7(b)].

At a higher level (y = 0.48 m) the maximum NO production rate is found closer to the inlet port, at z = 1.28 [(see Fig. 6(b)]. Once again, this region is located at the fuel-lean edge of the flame front shown in Fig. 5, except in a very small region where the profile crosses twice contour E. This contour corresponds to mixture fraction equal to 0.057 and it approximately indicates the flame front. The maximum NO production rate occurs in a region where the temperature profile exhibits steep gradients, with a maximum value of about 2500 K [Fig. 7(c)] and oxygen is available in significant amounts [Fig. 7(d)].

The maximum NO production rate continues to move towards the inlet port at higher levels, up to the burner level. Moving further upwards (y = 0.80 m), the maximum NO production rate is displaced downstream but still occurs near the flame front where the temperature of the post-combustion gases is high and oxygen is available [see Figs. 5, 6(c), 7(e), and 7f)].

Near the crown of the furnace (y = 1.12 m) a recirculation region is present and the temperature is lower. Therefore, the production rate is very small and the decomposition process may dominate [see Figs. 6(d) and 8].

It can be concluded that the NO production effect dominates in the outer edge of the flame where the temperatures are near their maximum values, where oxygen still attains high concentration values and where nitrogen is available in high concentrations (see [3]). Conversely, in regions where the temperature is still above 1400 K, where nitric oxide exists in

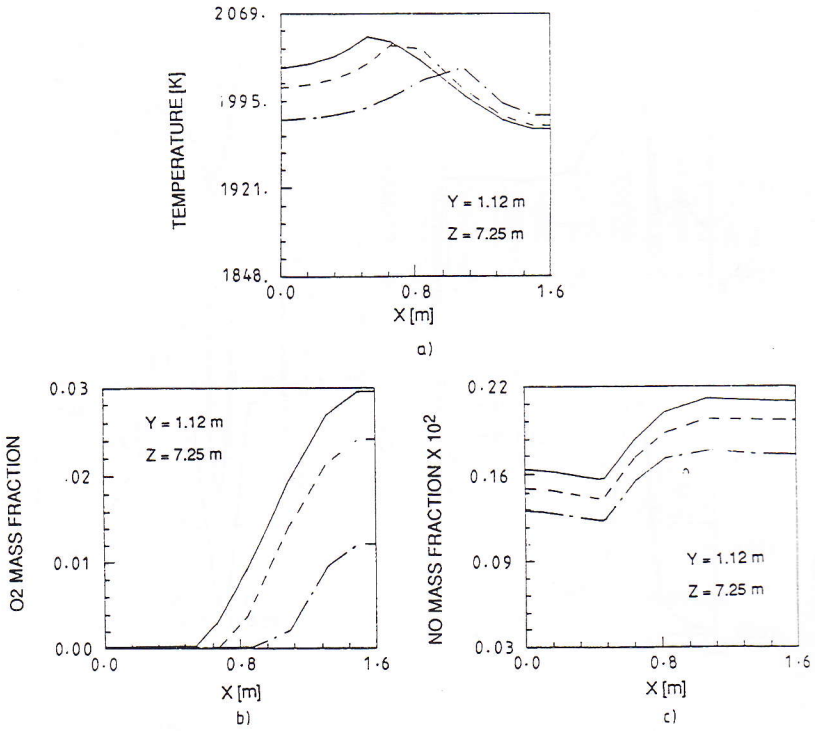

Fig. 8 Temperature profiles [K], oxygen mass fraction profiles [$Kg_{O2}Kg_{mix}^{-1}$] and NO mass fraction profiles [$Kg_{NO}Kg_{mix}^{-1}$] inside the furnace
—— 10 percent of excess air
----- 5 percent of excess air
—·—·— 0 percent of excess air

considerable concentrations and oxygen is still available, the NO decomposition effect, via the reverse reaction of the Zeldovich mechanism, plays an equal or dominant role compared with the production one.

The predicted NO emission values (see Table 2) are in the typical range values for industrial glass furnaces (2500 mg_{NO}/Nm^3 to 4500 mg_{NO}/Nm^3, where Nm^3 denotes cubic meter at standard conditions of pressure and temperature).

4.3 The Effect of the Excess-Air. The effects on the NO mass fraction and on the NO production rate of decreasing the excess-air level from 10 percent at the standard operating conditions to 5 percent and 0 percent are described below.

The reduction of the excess air, either to 5 percent or to the stoichiometric proportion, yields a decrease in the NO production rate, although the profiles are qualitatively similar (see Fig. 6). Oxygen concentration decreases as well, especially in the near flame-front region (see Fig. 7), where steep gradients of the properties can be noticed. Hence, as temperature is rather insensitive to the excess air level near the flame-front region [Figs. 7(*a*) and 7(*c*)], the oxygen concentration decrease, near this region, is the prime contributor to the reduction in the NO formation rate.

A rather different phenomenon occurs in the recirculation zone. In this region the thermal NO decomposition is equally or even more important than its formation [Fig. 6(*d*)]. Indeed, as temperatures are still high, the nitric oxide present in that zone reacts with available oxygen [see Fig. 8(*b*)]. The negative values of the reaction rates indicate that the NO decomposition dominates the mechanism. Furthermore, the decrease of the excess-air level leads to a reduction in the NO decomposition. Although this effect is opposite to the above mentioned reduction of the NO formation rate, in the near flame-front region, its magnitude is much smaller. Indeed, the global amount of NO leaving the furnace is diminished by decreasing the excess-air level.

Table 2 Predicted performance criteria of the furnace

RUN	Energy Input (KW)			Total heat flux to the glass	Outlet temperature	Outlet NO concentration	Outlet mass fraction of unburnt hydrocarbons
	AIR	FUEL	TOTAL	(KW)	(K)	(mg_{NO}/Nm^3)	
3	2466	3975	6441	1904	1968	3963	4.1×10^{-2}
4	2398	3975	6373	1891	1965	3866	4.9×10^{-2}
5	2284	3975	6259	1852	1957	3712	6.5×10^{-2}
6	2287	3975	6262	1739	1965	3535	4.1×10^{-2}
7	2646	3975	6621	2072	1971	4483	4.1×10^{-2}
8	2123	3426	5549	1609	1942	3789	3.0×10^{-2}

Table 2 illustrates some aspects of the comparative study of the furnace performance for the parameters under investigation. The results show that a reduction of the NO leaving the furnace can be accomplished by reducing the excess-air level. However, as a consequence of this reduction a smaller heat flux reaches the glass surface and a higher concentration of unburnt hydrocarbons leaves the furnace. As shown in Table 2, the value of the NO concentration leaving the furnace is reduced by 2.5 percent and 6.5 percent when the excess air is reduced to 5 percent and 0 percent, respectively.

4.4 The Effect of Air Preheating. Figure 9 shows selected temperature, NO production rate, and NO mass fraction profiles, along x direction, where the influence of air preheating is analyzed. It can be seen that the increase of air preheating results in a higher temperature level prevailing inside the furnace. This leads to an increase of the heat flux to the glass, as shown in Table 2, but the average outlet temperature is very similar for the three cases. The NO production rate increases as a result of the higher temperatures achieved. This is mainly due to the increase with temperature of the forward reaction R1 constant [3] which is directly proportional to the NO production rate. Consequently, the NO mass fraction inside the

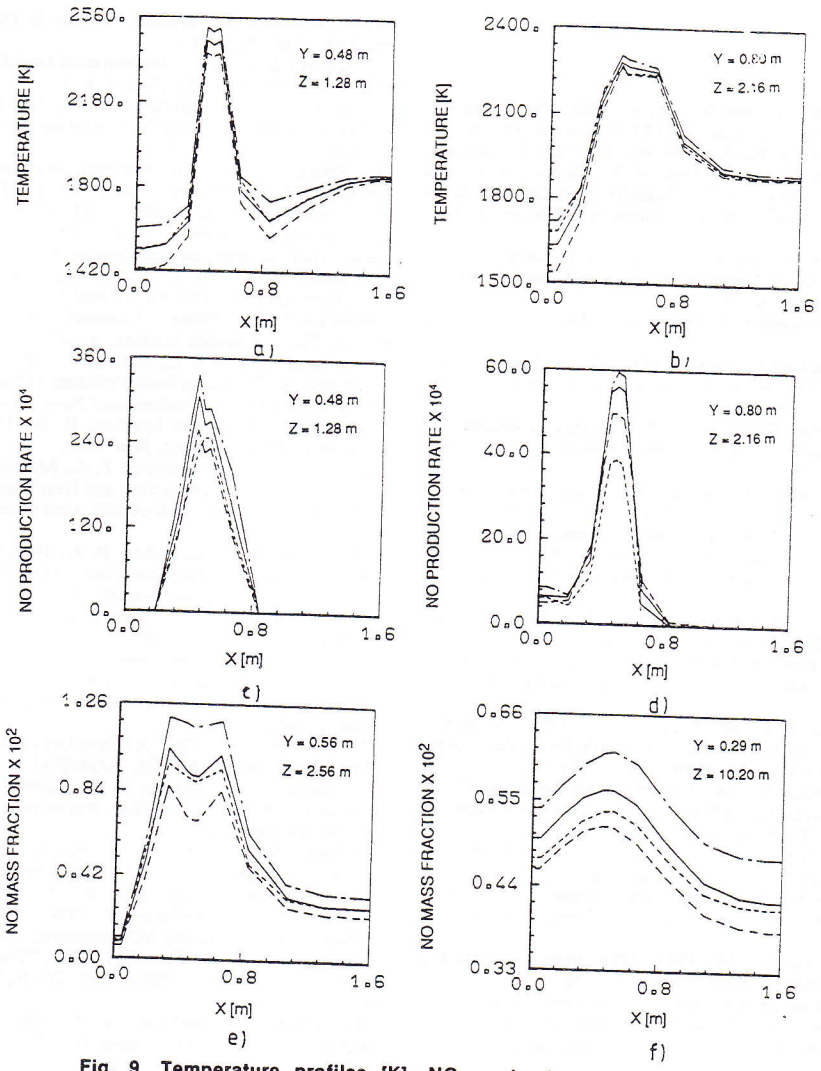

Fig. 9 Temperature profiles [K], NO production rate profiles [$kg_{NO}m^{-3}s^{-1}$] and NO mass fraction profiles [$Kg_{NO}Kg_{mix}^{-1}$] inside the furnace

—— standard operating conditions
— — — preheating = 1413 K
—·—·— preheating = 1613 K
····· 86 percent CH_4 + 14 percent N_2

furnace increases, as well as the NO emissions (see Table 2). The increase in NO emissions is quite large compared with the changes observed in the previous parametric study where the change of excess air was analyzed. On the other hand, the outlet mass fraction of unburnt hydrocarbons does not change at all with the air preheating because the excess air remains constant.

4.5 The Effect of Fuel Composition. The effect of changing the fuel from pure methane to a mixture of 86 percent methane and 14 percent nitrogen, a composition typical of natural gas, keeping the fuel flow rate and the air/fuel ratio constant, is also shown in Fig. 9. Although there is nitrogen available in the fuel when the mixture CH_4/N_2 is used, the air flow rate decreases because the excess air remains unchanged, and so the amount of nitrogen available decreases compared to standard operating conditions. The oxygen available decreases as well. Therefore, the NO production rate decreases, although the temperature field is very similar for the two fuels (see Fig. 9). The decrease in the NO production rate leads to a decrease in the NO mass fraction inside the furnace (Fig. 9) and at the outlet (Table 2).

5 Concluding Remarks

This paper has described the application of a very useful and general prediction procedure to a full-scale industrial glass melting furnace and has shown its ability to improve the design and operating conditions. The NO formation model relies on the Zeldovich mechanism and on the equilibrium assumption for the oxygen atom concentration. The results of previous studies suggest that the combustion aerodynamics and the heat transfer are probably fairly well predicted. The predicted NO emissions are consistent with recognized industry values although detailed comparisons are not possible at present due to the lack of reliable real data. The dominant region for NO formation in glass furnaces is the outer edge of the flame.

The reduction of the NO emissions is accomplished by decreasing the excess-air level. However, this reduction has the undesirable effects of decreasing the heat flux to the glass and increasing the amount of unburnt hydrocarbons leaving the furnace. The increase of air preheating leads to an increase of the heat flux to the glass but NO emissions increase significantly. When the fuel used is a mixture of methane and nitrogen rather than pure methane, the NO emissions decrease as well as the heat flux to the glass.

References

1 Carvalho, M. G., Oliveira, P., and Semião, V., 1988, "Modelling and Optimization of an Industrial Glass Furnace," *AIAA Progress in Astronautics and Aeronautics Series*. Vol. 113, p. 363, Kuhl, Bowen, Leyer and Borisov, eds.

2 Carvalho, M. G., Durão, D. E. G., Heitor, M. V., Moreira, A. L., and Pereira, J. C. F., 1988, "The Flow and Heat Transfer in an Oxy-Fuel Glass Furnace," 1st European Conference on Industrial Furnaces and Boilers, Lisbon, Portugal.

3 Carvalho, M. G., Semião, V., Lockwood, F. C., and Papadopoulos, C., 1990, "Predictions of Nitric Oxide Emissions from an Industrial Furnace," *Journal of Inst. of Energy*, March, p. 39.

4 Glassman, I., 1977, *Combustion*, Academic Press, Inc., Ltd., London, United Kingdom Edition.

5 Levy, A., 1982, "Unresolved Problems in SO_X, NO_X and Soot Control in Combustion," *Nineteenth Symposium (International) on Combustion*, The Combustion Institute, p. 1223.

6 Miller, J. A., and Bowman, C. T., 1989, "Mechanisms and Modelling of Nitrogen Chemistry in Combustion," *Prog. Energy Combust. Sci.*, Vol. 15, p. 287.

7 Zeldovich, Ya. B., Sadvnikov, P. Ya., and Frand-Kamenetskii, D. A., 1947, "Oxidation of Nitrogen in Combustion" (Tranl. by M. Shelef), Academy of Sciences of USSR, Institute of Chemical Physics, Moscow, Leningrad.

8 Fenimore, C. P., 1971, "Formation of Nitric Oxide in Premixed Hydrocarbon Flames," *Thirteenth Symposium (International) on Combustion*, The Combustion Institute, p. 373.

9 Westenberg, A. A., 1971, "Kinetics of NO and CO in Lean, Premixed Hydrocarbon Air Flames," *Comb. Sci. and Tech.*, Vol. 4, p. 59.

10 Bowman, C. T., 1973, "Kinetics of Nitric Oxide Formation in Combustion Processes," *Fourteenth Symposium (International) on Combustion*, The Combustion Institute, p. 729.

11 Flower, W. L., Hanson, R. K., and Kruger, C. H., 1975, "Kinetics of the Reaction of Nitric Oxide with Hydrogen," *Fifteenth Symposium (International) on Combustion*, The Combustion Institute, p. 823.

12 Peters, N., and Donnerhack, S., 1981, "Structure and Similarity of Nitric Oxide Production in Turbulent Diffusion Flames," *Eighteenth Symposium (International) on Combustion*, The Combustion Institute, p. 33.

13 Bowman, C. T., 1975, "Kinetics of Pollutant Formation and Destruction in Combustion," *Prog. Energy Combust. Sci.*, Vol. 1, p. 33.

14 Hayhurst, A. N., and Vince, I. M., 1980, "Nitric Oxide Formation from N_2 in Flames: the Importance of "Prompt" NO," *Prog. Energy Combust. Sci.*, Vol. 6, p. 35.

15 Hayhurst, A. N., and Vince, I. M., 1983, "The Origin and Nature of "Prompt" Nitric Oxide in Flames," *Comb. Flame*, Vol. 50, p. 41.

16 Drake, M. C., 1985, "Kinetics of Nitric Oxide Formation in Laminar and Turbulent Methane Combustion," Gas Research Institute Report, GRI-85/0271.

17 Turns, S. R., and Lovett, J. A., 1989, "Measurements of Oxides of Nitrogen Emissions from Turbulent Propane Jet Diffusion Flames," *Comb. Sci. and Tech.*, Vol. 66, p. 233.

18 Caretto, L. S., 1976, "Mathematical Modelling of Pollutant Formation," *Prog. Energy Combust. Sci.*, Vol. 1, p. 47.

19 Katsuki, M., and Mizutani, Y., 1977, "A Simplified Reactive Flow Model of Gas Turbine Combustors for Predicting Nitric Oxide Emissions," *Comb. Sci. and Tech.*, Vol. 17, p. 19.

20 Peters, N., 1978, "An Asymptotic Analysis of Nitric Oxide Formation in Turbulent Diffusion Flames," *Comb. Sci. and Tech.*, Vol. 17, p. 39.

21 Jones, W. P., and Priddin, C. H., 1978, "Predictions of the Flowfield and Local Gas Composition in Gas Turbine Combustors," *Seventeenth Symposium (International) on Combustion*, The Combustion Institute, p. 339.

22 Drake, M. C., Pitz, R. W., Correa, S. M., and Lapp, M., 1984, "Nitric Oxide Formation from Thermal and Fuel-Bound Nitrogen Sources in a Turbulent Nonpremixed Syngas Flame," *Twentieth Symposium (International) on Combustion*, The Combustion Institute, p. 327.

23 Ahmad, T., Plee, S. L., and Myers, J. P., 1985, "Computations of Nitric Oxide and Soot Emissions from Turbulent Diffusion Flames," ASME *Journal of Engineering for Gas Turbines and Power*, Vol. 107, p. 48.

24 Launder, B. E., and Spalding, D. B., 1972, *Mathematical Models of Turbulence*, Academic Press, New York.

25 Gosman, A. D., Lockwood, F. C., Megahed, I. E. A., and Shah, N. G., 1980, "The Prediction of the Flow and Heat Transfer in the Combustion Chamber of a Glass Furnace," AIAA 18th Aerospace Sciences Meeting, California, Paper No. 80-0016.

26 Williams, F. A., and Libby, P. A., 1980, "Some Implications of Recent Theoretical Studies in Turbulent Combustion," AIAA, Paper No. 80-0012.

27 Lockwood, F. C., and Naguib, A. S., 1975, "The Prediction of the Fluctuations in the Properties of Free, Round Jet, Turbulent Diffusion Flames," *Comb. Flame*, Vol. 24, p. 109.

28 Lockwood, F. C., and Shah, N. G., 1981, "A New Radiation Solution Method for Incorporation in General Combustion Prediction Procedures," *Eighteenth Symposium (International) on Combustion*, The Combustion Institute, p. 1405.

29 Truelove, J. S., 1976, "A Mixed Grey Gas Model for Flame Radiation," AERE Harwell Report No. HL 76/3448/KE.

30 Baulch, D. L., Drysdale, D. D., Horne, D. G., and Lloyd, A. C., 1973, "Evaluated Kinetic Data for High Temperature Reactions," Vols. 1, 2, and 3, Butterworth, London.

31 Drake, M. C., Correa, S. M., Pitz, R. W., Shyy, W., and Fenimore, C. P., 1987, "Superequilibrium and Thermal Nitric Oxide Formation in Turbulent Diffusion Flames," *Comb. Flame*, Vol. 69, p. 347.

32 Janicka, J., and Kollman, W., 1979, "A Prediction Model for T ɔulent Diffusion Flames Including NO Formation," AGARD CP-275.

33 Drake, M. C., and Blint, R. J., 1989, "Thermal NO_x in Stretched Laminar Opposed-Flow Diffusion Flames with $CO/H_2/N_2$ Fuel," *Comb. Flame*, Vol. 76, p. 151.

34 Hanson, R. K., and Salimian, S., 1984, *Combustion Chemistry*, W. C. Gardiner, Jr., ed., Springer-Verlag, New York, p. 361.